Earth Planets Space, **58**, 1025–1031, 2006

Long-distance traveling ionospheric disturbances caused by the great Sumatra-Andaman earthquake on 26 December 2004

Elvira I. Astafyeva and Edward L. Afraimovich

Institute of Solar-Terrestrial Physics SD RAS, P. O. Box 4026, Irkutsk, 664033, Russia

(Received February 17, 2006; Revised April 19, 2006; Accepted April 20, 2006; Online published September 16, 2006)

By using data from the GPS network, we observed exceptional intensive quasi-periodical perturbations of the total electron content (TEC) caused by the great Sumatra-Andaman earthquake on 26 December 2004. The time period of the variations was about 15 min, their duration was about 1 hour. The amplitude of the TEC oscillations exceeded the amplitude of "background" fluctuations in this range of periods by one order of magnitude, at a minimum. They were registered 2–7 hours after the main shock at a distance from 1000 to 5000 km, both on the northwest and northeast outward from the epicenter. The most probable source of the observed oscillations appeared to be a seismic airwave generated by the sudden vertical displacement of the Earth's surface near the epicenter.

Key words: TEC, traveling ionospheric disturbances, Sumatra-Andaman earthquake, GPS, seismic airwaves.

1. Introduction

Many publications have been devoted to the study of the ionospheric response to strong earthquakes (Davies and Baker, 1965; Tanaka *et al*., 1984; Liu *et al*., 2006; Calais and Minster, 1995; Afraimovich *et al*., 2001a, 2002, 2005, 2006; Ducic *et al*., 2003; Heki and Ping, 2005). Atmospheric waves excited by earthquakes include several types of waves (Pokhotelov *et al*., 1995; Ducic *et al*., 2003; Artru *et al*., 2004; Heki and Ping, 2005) and manifest themselves in the ionosphere as traveling ionospheric disturbances (TIDs).

First, the surface seismic waves while propagating, induce acoustic waves in the atmosphere. The amplitude of the atmospheric waves increases exponentially with altitude, and it leads to large vertical oscillations in the upper atmosphere and ionosphere (Golitsyn and Klyatskin, 1967; Row, 1967; Pokhotelov *et al*., 1995). An ionosphere response to Rayleigh surface waves propagation was detected by Doppler sounding and using GPS measurements as TIDs with a time period of 10–50 sec, propagated with a velocity of about of 3.5 km/s (Yuen *et al*., 1969; Artru *et al*., 2004; Ducic *et al*., 2003).

Then, 10–15 minutes after the main shock an ionosphere response to the shock-acoustic wave (SAW) propagation was detected nearby the epicenter of the earthquakes (Calais and Minster, 1995; Afraimovich *et al*., 2001a). Acoustic waves propagate upward from the focal area in a narrow cone of zenith angles with a velocity equal to the sound speed at these altitudes. The waves propagate into the atmosphere up to ionosphere altitudes where they are able to initiate an ionosphere plasma motion due to the collision interaction of neutral and charged particles. The parameters of SAW have been examined well using methods of TEC GPS-measurements (Calais and Minster, 1995; Afraimovich *et al*., 2001a; Heki and Ping, 2005). Such TEC perturbations are characterized by N-type waves and reflect the compression and decompression phases of certain acoustic waves (Afraimovich *et al*., 2001a).

Besides, sudden vertical displacements or tilting of the Earth's surface near the epicenter of the earthquakes excite acoustic waves propagating horizontally with a velocity about 300 m/s. Such waves are registered by ground microbarographs as air-pressure pulses with periods of about several minutes. These seismic airwaves can propagate for a long distance due to weak damping. Since energy spreads vertically, these waves can generate TIDs in the ionosphere F-layer (Bolt, 1964; Pokhotelov *et al*., 1995).

The great Sumatra-Andaman earthquake originated in the Indian Ocean off the western coast of northern Sumatra at 00:58:53 Universal Time (UT) on 26 December 2004. The magnitude (Mw) of the earthquake was estimated as 9.3. The epicenter with geographical coordinates of 3.29°N; 95.78°E was located in the Indian Ocean, southeast from the island of Sumatra. The land surface uplift is estimated to be up to 10 m (Bilham *et al*., 2005). The rupture due to the earthquake excited the most disastrous tsunami in recorded history (http://wwwneic.cr.usgs.gov/neis/).

This natural hazard has attracted attention of many scientists studying perturbations in solid earth, atmosphere, and ionosphere excited by the earthquake (Stein and Okal, 2005; Khan and Gudmundsson, 2005; Roder *et al*., 2005; Liu *et al*., 2006). Liu *et al*. found two types of ionosphere disturbances over Taiwan following the Sumatra-Andaman earthquake of 2004, using a network of digital Doppler sounders in Taiwan. The first disturbance was excited mainly by Rayleigh waves, which consists of a packet of short-period Doppler shift variations. The second disturbance is a W-shaped pulse with a duration of about 30 min. The most important result obtained by Liu *et al*. (2006) is the discovery for the first time, of the well-defined ionospheric response to the earthquake so far out of the epicenter (3500 km). But these data are not enough for understanding

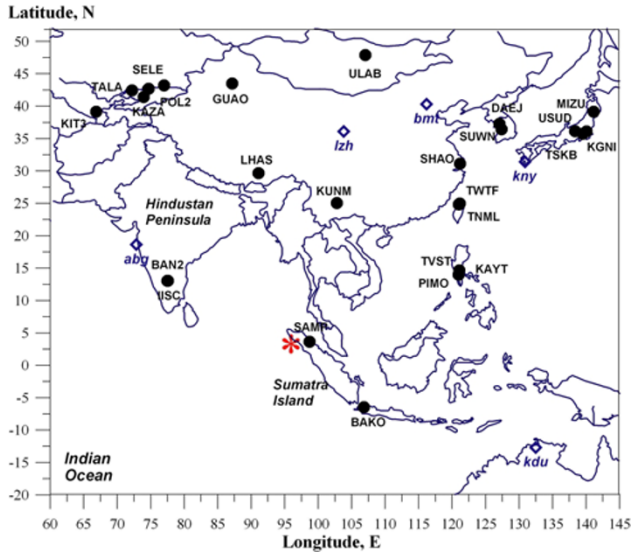

Fig. 1. Experimental geometry of GPS measurements during the earthquake of 26 December 2004. GPS-receivers are marked by heavy dots, the names of the sites are written nearby. Star shows the epicenter's location. Big diamonds indicate magnetic observatories, data of those we used in analysis of local geomagnetic activity.

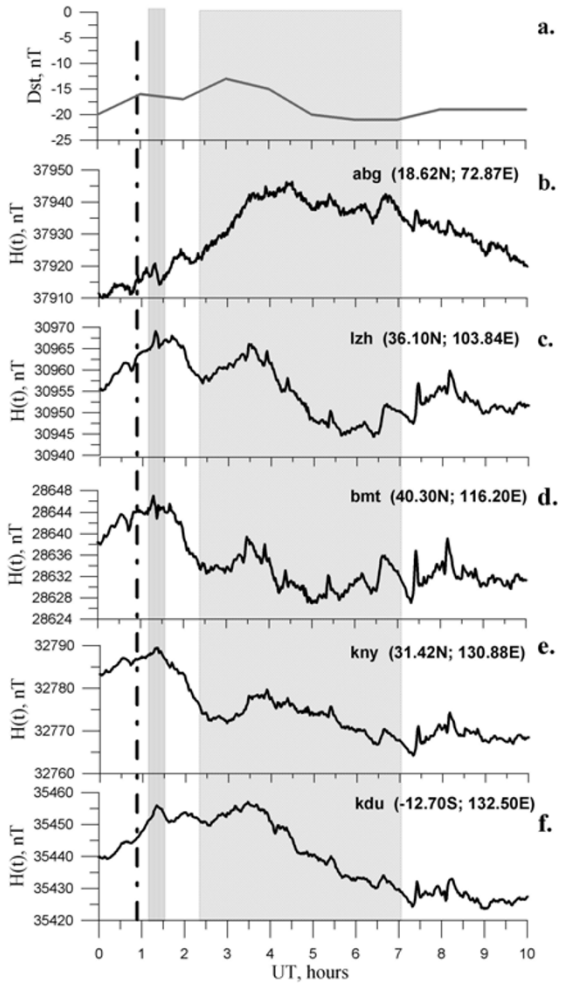

Fig. 2. Geomagnetic field Dst-variations (a) on 26 December 2004. $H(t)$-variations of the horizontal component of the geomagnetic field as recorded at the nearest magnetic observatories: (b) abg (18.62°N, 72.87°E), (c) lzh (36.1°N, 103.84°E), (d) bmt (40.3°N, 116.2°E), (e) kny (31.42°N, 130.88°E), (f) kdu (−12.7°N, 132.5°E). The time of the main shock is noted by a vertical dashed line, grey thin rectangle mark time period of the SAW response observation, grey thick rectangle indicate time period of the observation of intensive quasi-periodical oscillations.

the spatial characteristics of the ionosphere disturbance. To estimate the shape of the TIDs and the path of their propagation, data from spaced tools are necessary.

The aim of this paper is the investigation of the ionospheric response to the Sumatra-Andaman earthquake, both close to the epicenter and far from it, using GPS measurements. The geometry of TEC measurements during the earthquake on 26 December 2004 is presented in Fig. 1.

2. General Characteristics of the Experiment. Data Analysis

One can see from Figs. 2(a-f) that the geomagnetic situation on 26 December 2004 can be characterized as weakly disturbed: the Dst-variations were within −(22–13) nT and the Kp index varied from 2 to 3 (http://www.ukssdc.ac.uk/wdcc1/wdc_menu.html).

The data we used in our work are available in standard RINEX format with sampling intervals of 30 sec from site (http://sopac.ucsd.edu/cgi-bin/dbDataByDate.cgi).

The method of data processing has been described in detail in previous papers (Calais and Minster, 1995; Afraimovich *et al.*, 2001a). The standard GPS technology provides a means for wave-disturbance detection based on phase measurements of slant TEC I_s (Hofmann-Wellenhof *et al.*, 1992):

$$I_s = \frac{1}{40.308}\frac{f_1^2 f_2^2}{f_1^2 - f_2^2}[(L_1\lambda_1 - L_2\lambda_2) + \text{const} + nL], \quad (1)$$

where $L_1\lambda_1$ and $L_2\lambda_2$ are additional paths of the radio signal caused by the phase delay in the ionosphere, (m); L_1 and L_2 represent the number of phase rotations at the frequencies f_1 and f_2; λ_1 and λ_2 stand for the corresponding wavelengths, (m); const is the unknown initial phase path caused by an unknown number of total phase rotations along the line-of-sight (LOS); and nL are errors in determining the phase path. TEC I_s is measured in m^{-2}; const 40.308 has the dimension (m^3/s^2).

Phase measurements in the GPS technology can be made with a high degree of accuracy corresponding to the error of TEC determination of at least 10^{14} m^{-2} when averaged on a 30-sec time interval, with some uncertainty of the initial value of TEC, however (Hofmann-Wellenhof *et al.*, 1992). The unit of TEC, which is equal to 10^{16} m^{-2} (TECU) and is commonly accepted in the literature, will be used in the paper.

To normalize the response amplitude, we converted the slant TEC $I_s(t)$ to an equivalent vertical value $I(t)$ (Klobuchar, 1986).

3. TEC Response to Acoustic-Shock Waves

Figure 3 presents TEC perturbations due to SAW propagation recorded at the nearest to the earthquake epicenter GPS site SAMP. To select the TEC response to shock-

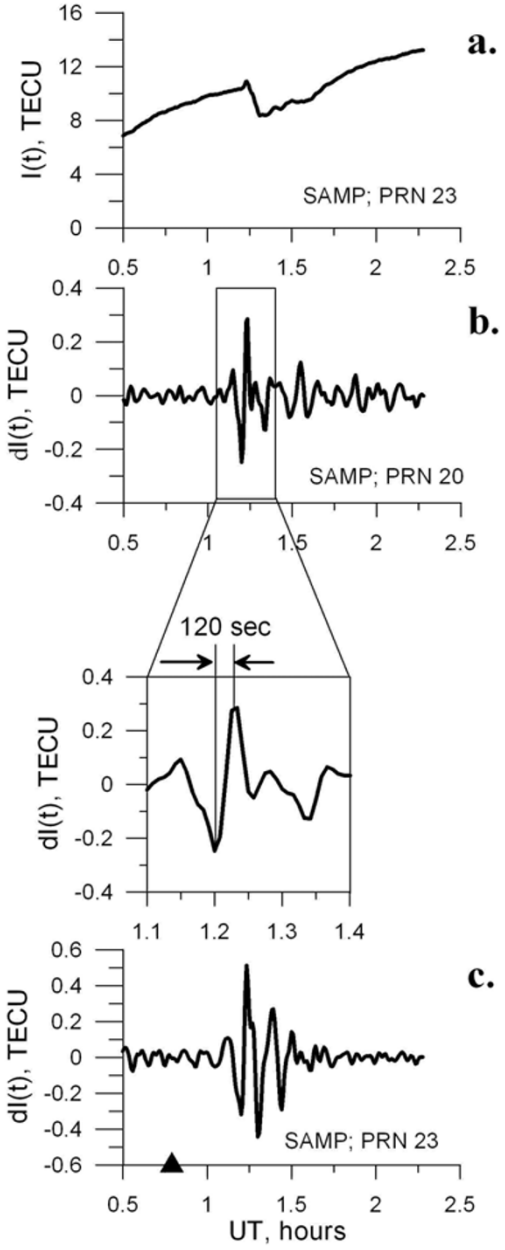

Fig. 3. Time dependencies of the initial TEC series $I(t)$ for site SAMP – panel (a), and filtered in the range of 2–10 min TEC series $dI(t)$ – (b), (c). The moment of the main shock is marked by shaded triangle.

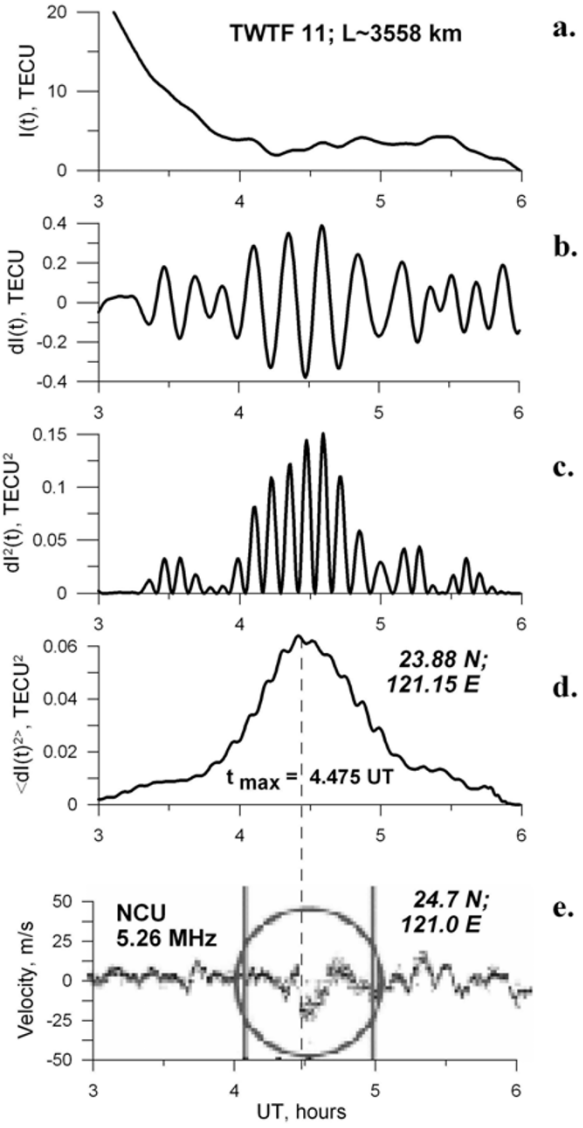

Fig. 4. GPS data processing at the registration TEC oscillations: estimating of the time of maximal amplitude of TEC response (a–d). (e) digital Doppler sounder record of the ionospheric disturbance obtained at station NCU by Liu *et al*. (2006).

acoustic wave propagation from the initial TEC series $I(t)$, we used moving-mean filtering in the range periods of 2–10 min. The TEC response was observed 13 min after the main shock, in the form of N-waves with a time duration of about 240 sec (120 sec from the first minima to the first maxima of response - see Fig. 3(b), rectangle fragment). The amplitude is about 0.3–0.4 TECU and exceeds the background TEC fluctuation intensity in this range of periods (Afraimovich *et al*., 2001b).

Unfortunately, we did not succeed in determining the wave-front parameters and velocity of the SAW propagation due to the lack of data. For such purposes we need data of no less than three GPS receivers (Afraimovich *et al*., 2001a, 2002).

4. Quasi-Periodical TEC Oscillations Far from the Earthquake Epicenter

The most important and the most interesting result of our work is in evident registration of the ionospheric response to the earthquake not only at the nearest GPS sites but also at outlying ones (at a distance of more than 5000 km), 2–7 hours after the earthquake. We observed exceptional intensive quasi-periodical TEC oscillations with the time period T of about of 15 min and a duration of the order of 60 min. It should be noted that we observed such oscillations at GPS sites both northwest and northeast of the epicenter (from -20°N to 50°N latitude and from 60°E to 145°E longitude; Fig. 1, Table 1, 23 GPS sites).

To select quasi-periodical TEC oscillations from the initial TEC series $I(t)$, we used moving-mean filtering in the range periods of 10–20 min.

Figures 4(a) and (b) demonstrate vertical TEC $I(t)$ and filtered TEC variations $dI(t)$ at TWTF site (about 3680

Table 1. Velocity and periods of quasi-periodical TEC oscillations after the Sumatra-Andaman earthquake.

N	SITE	Lat., °N	Lon.,°E	PRN	L, km	V, m/s	T, min
Northeast, $\langle V\rangle$=295±38 m/s, $\langle T\rangle$= 15.15 min, $\langle\Lambda\rangle$= 274 km							
1	KAYT	13.987	120.978	11	2915	343	16.0
2	TVST	14.034	121.002	11	2918	344	16.0
3	PIMO	14.636	121.078	11	2919	376	16.5
4	TNML	24.798	120.987	11	3536	300	14.0
5	TWTF	24.953	121.164	11	3558	302	14.0
6	SHAO	31.099	121.200	31	3623	223	13.0
7	SUWN	37.276	127.054	31	4146	268	15.5
8	DAEJ	36.399	127.374	31	4219	265	15.0
9	ULAB	47.865	107.052	31	4909	275	15.5
10	KGNI	35.711	139.488	31	5132	286	15.0
11	USUD	36.133	138.362	31	5291	278	14.0
12	TSKB	36.106	140.087	31	5293	283	16.0
13	MIZU	39.135	141.134	31	5707	292	16.5
Northwest, $\langle V\rangle$=205±38 m/s, $\langle T\rangle$=16.25 min, $\langle\Lambda\rangle$= 203 km							
1	IISC	13.021	77.570	11	1951	154	17.0
2	BAN2	13.036	77.512	11	1955	159	17.0
3	LHAS	29.657	91.104	11	2719	159	17.5
4	KUNM	25.029	102.797	11	3087	178	16.0
5	GUAO	43.472	87.177	31	4426	273	17.0
6	KAZA	41.383	73.942	31	4767	240	15.5
7	SELE	43.178	77.016	31	4835	223	15.0
8	POL2	42.679	74.694	31	4878	220	15.5
9	KIT3	39.135	66.885	31	4948	210	16.0
10	TALA	42.445	72.210	31	4957	228	16.0

km from the epicenter). One can see in Fig. 4(a) quasi-periodic TEC oscillations in the form of a wave packet with a duration of about 1 hour and with a typical period T of about of 15 min. The oscillation amplitude exceeds, by one order of magnitude, the intensity of the background TEC fluctuations of this range of periods (Afraimovich *et al.*, 2001b).

TEC oscillations recorded at the sites north-east from the epicenter are shown in Figs. 5(a-e). Figures 5(f, g) show TEC oscillations registered north-west from the epicenter. The panels are placed as a distance L between the earthquake's epicenter and the corresponding GPS sites increases. The distance L was estimated from the great circle length. The names of the sites, PRN of satellites, and the mean value of distance from the epicenter $\langle L\rangle$ are shown in the panels. Obvious resemblance of the shape of these oscillations as well as systematical lagging of the wave-packet maxima can be noticed. Therefore, we conclude that the observed TEC oscillations appeared to be the TID propagated outward from the source.

As one can see from Figs. 5(b, e, g), it is difficult to estimate the comparative lagging between TEC oscillations at near-spaced points of observation (we colored them light gray, gray and black curves). Therefore, time dependencies of power of TEC variations $dI(t)^2$ were determined from $dI(t)$ for analysis of the envelope characteristics. Figure 4 illustrates the detailed procedure for calculation of the envelope of TEC oscillations. Figure 4(b) demonstrates TEC variations $dI(t)$ after the linear trend removing and filtering and Figure 4(c) shows $dI(t)^2$. The envelope $dI(t)^2$ (Fig. 4(d)), was smoothed with the time window of 40 min. The moment of the maximal value $t_{\max} = 4.475$ UT of the envelope of $dI(t)^2$ is noted by vertical line.

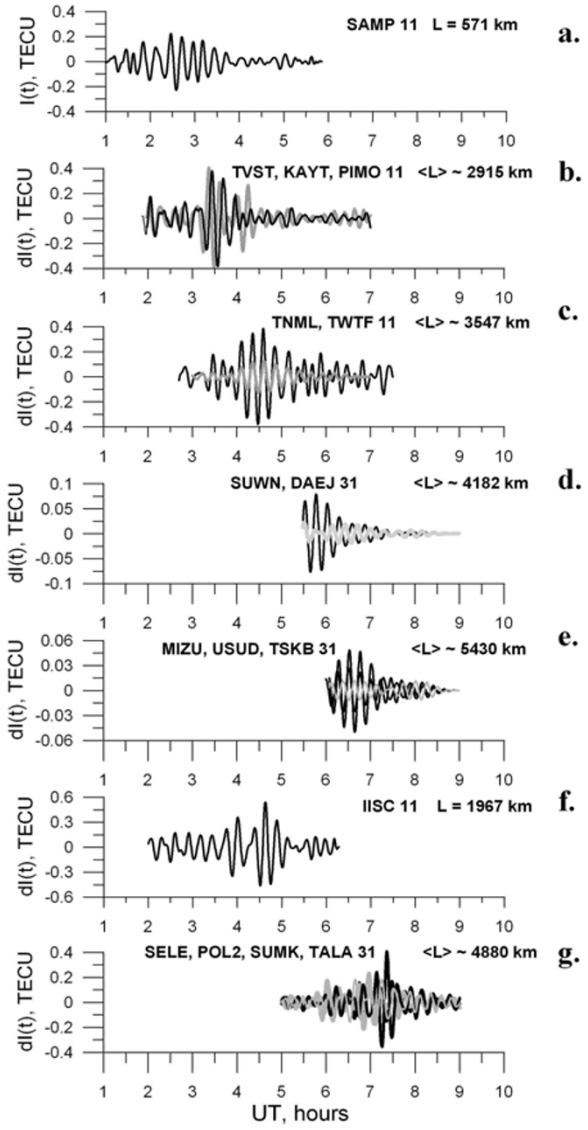

Fig. 5. TEC oscillations $dI(t)$ registered at different distance L from the epicenter. The TEC oscillations for the near-spaced GPS receivers, located in Philippines, Taiwan, Korea, Japan, and Middle Asia, are shown in panels (b, c, d, e, g) and are marked by light gray, gray and black colors.

The velocity of the propagation of TIDs can be calculated using the dependence of the envelope maximal lagging $t_{\max}$ from the distance L:

$$V = \frac{L}{t_{\max} - t_d - t_0}, \qquad (2)$$

where t_0 is the moment of the main shock and t_d is the lagging of acoustic perturbation propagation from the ground to the ionosphere F-layer height. In our calculations we take $t_d = 13$ min which corresponds to the time of lagging of the ionosphere response registered nearby the epicenter of the earthquake (see Section 3).

We calculated a horizontal component of a group velocity V (from here on, for the sake of convenience of statement, we simply note "group velocity") of the TID's propagation for all GPS sites using Eq. (2) (Table 1). The mean value of the group velocity V of TIDs at a distance from 2000 to 5000 km in the northeast is 295 ± 38 m/s and 205 ± 38 m/s on the northwest.

Another method of determining TID parameters is based on the method proposed in a previous paper (Afraimovich *et al*., 2001a). Due to the coordinates of spaced GPS sites being known, we can determine the group velocity V and the direction α of the TID wave vector **K** from time shifts between values $t_{\max}$ for sites. The orientation α of the wave vector **K** is defined clockwise from the north.

Thus, for GPS array [MIZU, TWTF, TVST], the group velocity V is 292 m/s and the propagation azimuth α is 41°; for GPS array [MIZU, TWTF, SUWN], these values are 293 m/s and 72°, respectively. For GPS array [SELE, LHAS, BAN2], located to the north-northwest from the epicenter, the group velocity equals 210 m/s and the azimuth α is 350°; for GPS array [KIT3, LHAS, BAN2], these values are 176 m/s and 344°, respectively. The velocity values, calculated using spaced GPS sites, coincide well with those calculated from the dependence of the envelope maximal lagging $t_{\max}$ from the distance L (Table 1). The propagation direction of TID α is opposite to the direction toward the earthquake's epicenter.

The mean value of the wavelength of TIDs $\Lambda = \langle V \rangle \langle T \rangle$ at a distance from 2000 to 5000 km in the northeast, is 274 and 209 km for those on the northwest (Table 1). So detected intensive quasi-periodical TEC disturbances are medium-scale TIDs (Francis, 1974; Afraimovich *et al*., 2003).

We worked out a question of the source of the medium-scale TIDs we observed. First of all, we did not find other possible sources of the oscillations such as solar flares (Afraimovich, 2000) (http://www.sel.noaa.gov/ftpdir/indices/) meteorological phenomena (Hung *et al*., 1978; Huang *et al*., 1985) (http://www.solar.ifa.hawaii.edu/Tropical), industrial explosions or rocket launches (http://www.cosmoworld.ru/spaceencyclopedia/index.shtml).

Second of all, there were no significant variations of the H-component of the geomagnetic field, which could probably have caused TIDs (Afraimovich *et al*., 2001, 2004a). We examined local geomagnetic activity using data from near-lying magnetic observatories, marked by diamonds in Fig. 1. One can see from Figs. 2(b, f) that amplitude of the H-component of the geomagnetic field on 26 December, did not exceed 7 nT and could hardly have caused significant TEC variations.

Another important point is the occurrence of TEC oscillations with similar parameters, but were not excited by the source of the TIDs we observed. Figure 6 presents the distribution $N(t)$ of a number of data series (with a time duration of about 2 h) of TEC variations in a time period range 10–20 min with a rms value of more than 0.1 TECU; this threshold exceeds the background TEC variations' rms more than 10 times (Afraimovich *et al*., 2001b). We detected 41 patterns from a possible 7920 data series (87 GPS sites) for the region (−60°N–+60°N and 60°E–160°E) during the whole day of 26 December 2004. The maximal number of patterns was observed from 02:00 to 08:00 UT; among the 41 patterns, we found only 23 quasi-periodic TEC variations of the wavepacket type. Besides, we did not detect such intensive quasi-periodic TEC oscillations after 12:00 UT.

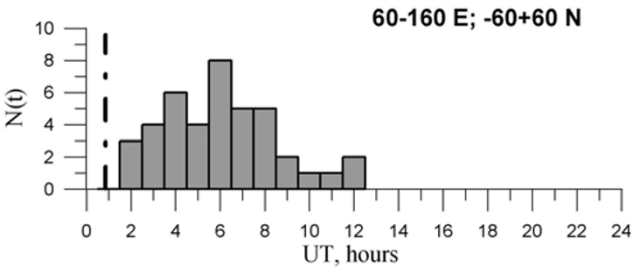

Fig. 6. The distribution $N(t)$ of the number of TEC oscillations detected for all the day on 26 December.

Hence, our observations show that the TIDs we detected are the response of the ionosphere to the main shock of the earthquake, but not background TEC perturbations, and they were not caused by other possible sources.

5. Discussion and Conclusion

After the great Sumatra-Andaman earthquake, we observed two types of perturbations in TEC variations. About 13 min after the earthquake at the nearest to the earthquake's epicenter GPS sites, we detected N-type variations of TEC with a time period of about of 240 s. Such variations are considered to be the manifestation in the ionosphere of shock-acoustic waves. The parameters of TEC response to SAW, excited by the main shock of the earthquake, agree well with the results of earlier papers devoted to the study of ionospheric effects of earthquakes. Such ionospheric disturbances propagate no further than 1000 km with a velocity of about 1000 m/s (Calais and Minster, 1995; Afraimovich *et al*., 2001a, 2002, 2005, 2006; Heki and Ping, 2005).

Besides, we observed medium-scale TIDs in the form of intensive quasi-periodical TEC variations with a time period of about of 15 min and duration in the order of 1 hour. The amplitude of TIDs exceeded the amplitude of "background" TEC fluctuations by one order of magnitude, as a minimum and practically did not change while propagating. Such variations were observed 2–7 hours after the main shock from 1000 to 5000 km, both on northwest and northeast outward from the epicenter. The horizontal component of the group velocity of TIDs propagation reached 295 ± 38 m/s for the GPS receivers located on the northeast out of the epicenter and 205 ± 38 m/s for those on the northwest. As one can see from Table 1, the values of a horizontal propagation velocity of TIDs north-eastward and north-westward are different. This fact could be explained by different conditions for seismic air wave propagation. However, detailed investigation of this problem is beyond the scope of this paper.

We compared our data with that obtained by Liu *et al*. (2006). Using a network of digital Doppler sounders in Taiwan, Liu *et al*. (2006) found an ionospheric disturbance in the form of a W-shaped pulse with a duration of about

30 min, following the M9.3 Sumatra earthquake of 26 December 2004. Figure 4(e) shows the velocity of reflection height changes for the Doppler sounding signals 5.26 MHz observed at the Doppler sounder station NCU (24.7°N; 121.0°E). The mean value of reflection height was at about 200 km altitude. TEC variations at TWTF, the nearest GPS site to the Doppler sounder station NCU (the coordinates of subionospheric point for PRN11 at 300 km altitude equals 23.88°N; 121.15°E), are shown in Fig. 4(b). One can see from Fig. 4 that the time of arrival of the *W*-shaped Doppler pulse (Fig. 4(e) coincides with the moment of the maximal value $t_{\max} = 4.475$ UT of the envelope of the TEC wavepacket for GPS site TWTF, PRN11 (noted by the vertical line in Figs. 4(d, e)). Thus, from the comparison above, one can conclude that the very same TID due to the earthquake were detected using different methods of radiosounding. Moreover, Liu *et al*. (2006) found that ionospheric disturbances traveled over Taiwan with a velocity of about 360 m/s; this value agrees with our data for the north-east direction (Table 1).

The difference between the forms and duration of the HF Doppler shift signal and TEC response (Figs. 4(b, e)) can be explained by different experimental tools and, therefore, by some peculiarities of recourse to observations. It is known that during HF Doppler shift measurements, the sensitivity field to ionospheric disturbances coincide with the area of HF signal reflection. The size of this area is very small and close to a characteristic size of the first Fresnel zone radius (3–4 km for 5.26 MHz). Meantime, TEC variations show changes within the region of the main maximum of electron concentration with a characteristic size of the order of 100–300 km (Afraimovich *et al*., 2003, 2004a, 2005, 2006). Therefore, the duration of HF Doppler shift response during wavepacket propagation is less than the duration of TEC perturbation (Afraimovich *et al*., 2004b). At the same time, the period of the TID recorded both by the HF Doppler sounder and GPS receiver is about 15 min, as one can see from Figs. 4(b, e)).

The question of the source of the observed TEC oscillation is not clear yet. It is known that TIDs can propagate without significant attenuation and changing their shape or losing their coherence no farther than 3–5 wavelengths (Francis, 1974). Indeed, intensive large-scale TIDs with wavelengths of more than 3000 km and time periods of 1–2 hrs were detected after nuclear explosions (Obayashi, 1963; Oksman and Kivenen, 1965) and the explosion of Mount St. Helens on 18 May 1980 (Roberts *et al*., 1982). These waves propagated at large distances, which exceed 10000–15000 km, without significant attenuation. Medium-scale TIDs can propagate no farther than 1000 km (Francis, 1974). Using the data of the global GPS receiver network for 1998–2001, Afraimovich *et al*. (2003) found that the radius of spatial correlation of medium-scale TIDs with time periods in the range 10–20 min does not exceed 500–600 km, that is verified by measurement of the conclusion of Francis's theory (1974).

However, in this work we observed medium-scale TIDs at a distance of more than 5000 km from the earthquake's epicenter. One can calculate that the TIDs were observed at a distance of more than 15 wavelengths (about 200–300 km; see Table 1). Some earlier papers reported on the registration of TIDs with a period range 5–20 min at large distances (Bolt, 1964; Davies and Baker, 1965; Liu *et al*., 1982, 2006).

One possible explanation of this phenomenon is the traveling sources of the TIDs we detected, such as a seismic air wave (Press and Harkrider, 1962; Liu *et al*., 1982). It is known that sudden vertical displacement or tilting of the Earth's surface near the epicenter of the earthquake can generate a seismic airwave, recorded as a sharp air-pressure fluctuation in the time period of about 5 min in barograms. Thus, 2.9 h after the Alaskan earthquake on 28 March 1964, an atmospheric wave with a period of 3 min and a velocity of 317 m/s was recorded at Berkley, 3130 km away from the epicenter (Bolt, 1964). It was also previously reported on the pressure pulses propagating in the atmosphere after such natural events as the Krakatoa volcanic eruption (Pekiris, 1939) and the Siberian meteoritic impact (Whipple, 1930). Liu *et al*. (1982) observed global atmospheric perturbations due to the 18 May 1980, eruption of Mount St. Helens.

Thus, the seismic airwave, generated by the vertical displacement of the Earth's surface near the epicenter, most likely appeared to be the source of the quasi-periodical TEC oscillations far off the earthquake epicenter. The detected TIDs are ionospheric responses to seismic airwaves, traveling for long distances without significant damping and changes of oscillation spectrum. So, we registered not initial medium-scale TIDs, excited by the earthquake main shock, but "secondary" TIDs, generated by traveling airwaves. This is the only one explanation of the TIDs characteristics we observed: the propagation velocity and TEC response shape constancy, and weak damping of TEC oscillations amplitude.

Acknowledgments. We are grateful to Profs. E. A. Ponomarev and V. V. Kuznetzov for their interest in this work and for fruitful discussions. The authors wish to thank members of the Scripps Orbit and Permanent Array Center (SOPAC) for the RINEX files used in this paper. The work was supported by the SD RAS collaboration project No. 3.24 and RFBR grant 05-05-64634.

References

Afraimovich, E. L., GPS global detection of the ionospheric response to solar flares, *Radio Science*, **35**(6), 1417–1424, 2000.

Afraimovich, E. L., N. P. Perevalova, A. V. Plotnikov, and A. M. Uralov, The shock-acoustic waves generated by the earthquakes, *Annales Geophysicae,* **19**, 395–409, 2001a.

Afraimovich, E. L., E. A. Kosogorov, O. S. Lesyuta, I. I. Ushakov, and A. F. Yakovets, Geomagnetic control of the spectrum of traveling ionospheric disturbances based on data from a global GPS network, *Annales Geophysicae,* **19**, 723–731, 2001b.

Afraimovich, E. L., V. V. Kirushkin, and N. P. Perevalova, Determination of the characteristics of ionospheric disturbance in the near zone of the earthquake epicenter, *J. Communications Technology and Electronics,* **47**, 739–747, 2002.

Afraimovich E. L., N. P. Perevalova, and S. V. Voyeikov, Traveling wave packets of total electron content disturbances as deduced from global GPS network data, *J. Atmos. Solar-Terr. Phys*., **65**, 1245–1262, 2003.

Afraimovich, E. L., E. I. Astafieva, V. V. Demyanov, I. F. Gamayunov, T. N. Kondakova, S. V. Voeykov, and B. Tsegmed, Ionospheric, Geomagnetic Variations and GPS Positioning Errors During the Major Magnetic Storm on 29–31 October 2003, *International Reference Ionosphere News*, **11**(3, 4), 10–14, 2004a.

Afraimovich, E. L., Yu. B. Bashkuev, O. I. Berngardt, A. V. Gatsutsev, M. G. Dembelov, B. G. Shpynev, V. A. Kobzar, D. S. Kushnarev, V.

Yu. Musin, P. Yu. Pushkin, and N. P. Perevalova, Detection of Traveling Ionospheric Disturbances from the Data of Simultaneous Measurements of the Electron Concentration, Total Electron Content, and Doppler Frequency Shift at the ISTP Radiophysical Complex, *Geomagnetism and Aeronomy*, **44**(4), 463–475, 2004b.

Afraimovich, E. L., E. I. Astafieva, and V. V. Kirushkin, Ionospheric Disturbance in the Near-Region of an Earthquake Epicenter on 25 September 2003, *Radiophysics and Quantum Electronics*, **48**(4), 299–313, 2005.

Afraimovich, E. L., E. I. Astafieva, and V. V. Kirushkin, Localization of the source of ionospheric disturbance generated during an earthquake, *International J. Geomagnetism and Aeronomy*, **6**, GI2002, doi:10.1029/2004GI000092, 2006.

Artru, J., T. Farges, and P. Lognonne, Acoustic waves generated from seismic surface waves: propagation properties determined from Doppler sounding observations and normal-mode modeling, *Geophys. J. Int.*, **158**, 1067–1077, 2004.

Bilham, R., R. Engdahl, N. Feldl, and S. P. Satyabala, Partial and complete rupture of the Indo-Andaman plate boundary 1847–2004, *Seism. Res. Lett.*, **76**, 299–311, 2005.

Bolt, B. A., Seismic air waves from the great 1964 Alaskan earthquake, *Nature*, **202**, 1094–1095, 1964.

Calais, E. and J. B. Minster, GPS detection of ionospheric perturbations following the January 1994, Northridge earthquake, *Geophys. Res. Lett.*, **22**, 1045–1048, 1995.

Davies, K. and D. M. Baker, Ionospheric effects observed around the time of the Alaskan earthquake of March 28, 1964, *J. Geophys. Res.*, **70**, 2251–2253, 1965.

Ducic, V., J. Artru, and P. Lognonne, Ionospheric remote sensing of the Denali Earthquake Rayleigh surface wave, *Geophys. Res. Lett.*, **30**(18), 1951, doi:10.1029/2003GL017812, 2003.

Francis, S. H., A theory of medium-scale traveling ionospheric disturbances, *J. Geophys. Res.*, **79**(34), 5245–5260, 1974,

Golitsyn, G. S. and V. I. Klyatskin, Atmosphere oscillations caused by Earth's surface displacement, *Izvestiya, Atmospheric Oceanic Physics*, **3**, 1044–1052, 1967.

Heki, K. and J.-S. Ping, Directivity and apparent velocity of the coseismic ionospheric disturbances observed with a dense GPS array, *Earth Planet Sci. Lett.*, **236**, 845–855, 2005.

Hofmann-Wellenhof, B., H. Lichtenegger, and J. Collins, *Global Positioning System: Theory and Practice*, Springer-Verlag, Vienna, New York, 327 p, 1992.

Huang, Y.-N., C. Kang, and S.-W. Chen, On the detection of acoustic-gravity waves generated by typhon by use of real time HF Doppler frequency shift sounding system, *Radio Sci.*, **20**, 897–906, 1985.

Hung, R. G., T. Phan, and R. E. Smith, Observation of gravity waves during the extreme tornado outbreak of 3 April 1974, *J. Atmos. Solar-Terr. Phys.*, **40**, 831–843, 1978.

Klobuchar, J. A., Ionospheric time-delay algorithm for single-frequency GPS users, *IEEE Transactions on Aerospace and Electronics System*, **23**(3), 325–331, 1986.

Khan, S. A. and O. Gudmundsson, GPS analyses of the Sumatra-Andaman earthquake, *EOS, Transactions, AGU*, **86**(9), 89–100, 2005.

Liu, C. H., J. Klostermeyer, K. C. Yeh, T. B. Jones, T. Robinson, O. Holt, R. Leitinger, T. Ogawa, K. Sinno, S. Kato, T. Ogawa, A. J. Bedard, and L. Kersley, Global dynamic responses of the atmosphere to the eruption of mount St. Helens on May 18, 1980, *J. Geophys. Res.*, **87**(A8), 6281–6290, 1982.

Liu, J. Y., Y. B. Tsai, S. W. Chen, S. P. Lee, Y. C. Chen, H. Y. Yen, W. Y. Chang, and C. Liu, Giant ionospheric disturbances excited by the M9.3 Sumatra earthquake of 26 December 2004, *Geophys. Res. Lett.*, **33**, L02103, doi:10.1029/2005GL023963, 2006.

Obayashi, T., Upper atmospheric disturbances due to high altitude nuclear explosions, *Planet. Space Sci.*, **10**, 47–63, 1963.

Oksman, J. and M. Kivinen, Ionospheric gravity waves caused by nuclear explosions, *Geophysica*, **9**, 119–130, 1965.

Pekeris, C. L., The propagation of a pulse in the atmosphere, *R. Soc. London Ser. A*, **A171**, 434–449, 1939.

Pokhotelov, O. A., M. Parrot, E. N. Fedorov, V. A. Pilipenko, V. V. Surkov, and V. A. Gladychev, Response of ionosphere to natural and man-made acoustic sources, *Annales Geophysicae*, **13**, 1197–1210, 1995.

Press, F. and D. Harkrider, Propagation of acoustic-gravity waves in the atmosphere, *J. Geophys. Res.*, **67**, 3889–3908, 1962.

Roberts, D. H., J. A. Klobuchar, P. F. Fougere, and D. H. Hendrickson, A large-amplitude traveling ionospheric disturbance produced by the May 18, 1980, explosion of Mount St. Helens, *J. Geophys. Res.*, **87**(A8), 6291–6301, 1982.

Roder, H., T. Braun, W. Schunmann, E. Boschi, R. Buttner, and B. Zimanovsky, Great Sumatra earthquake registers on electrostatic sensor, *EOS, Transactions AGU*, **86**, 45, 449–450, 8 November 2005.

Row, R. V., Acoustic-gravity waves in the upper atmosphere due to a nuclear detonation and an earthquake, *J. Geophys. Res.*, **72**, 1599–1610, 1967.

Stein, S. and E. A. Okal, Speed and size of the Sumatra earthquake, *Nature*, **434**, 581–582, 2005.

Tanaka, T., T. Ichinose, T. Okuzawa, T. Shibata, Y. Sato, C. Nagasawa, and T. Ogawa, HF-Doppler observations of acoustic waves excited by the Urakawa-Oki earthquake on 21 March 1982, *J. Atmos. Terr. Phys.*, **46**, 233–245, 1984.

Whipple, F. J. W., The great siberian meteor and the waves, seismic and aerial, which it produced, *Quart. J. Roy. Met. Soc.*, **56**, 287–304, 1930.

Yuen, P. C., P. F. Weaver, R. K. Suzuki, and A. S. Furumoto, Continuous travelling coupling between seismic waves and the ionosphere evident in May 1968 Japan earthquake data, *J. Geophys. Res.,* **74**(9), 2256–2264, 1969.

E. I. Astafyeva and E. L. Afraimovich (e-mail: Afra@iszf.irk.ru)